Monte Carlo uncertainty and sensitivity analysis of the CACM chemical mechanism

Marco A. Rodriguez and Donald Dabdub

Department of Mechanical and Aerospace Engineering, University of California, Irvine, Irvine, California, USA

Received 3 December 2002; accepted 25 March 2003; published 2 August 2003.

[1] This paper presents a global uncertainty and sensitivity analysis of the Caltech Atmospheric Chemistry Mechanism (CACM). Emphasis is placed on the characterization of uncertainties for product concentrations that constitute secondary organic aerosol (SOA) in CACM. The sensitivity analysis of the chemical mechanism is performed using Monte Carlo techniques combined with Latin hypercube sampling. Uncertainties in rate parameters are propagated through box model simulations with CACM for three different summer cases. Cases studied cover a range of initial concentrations of reactive organic gases and nitrogen oxides that represent episodes of high ozone levels in polluted urban areas. In addition to estimated uncertainties of gas-phase SOA precursor concentrations, similar calculations are performed for O₃, HCHO, H₂O₂, and peroxyacetyl nitrate (PAN). Results indicate that SOA precursor concentrations predicted using nominal CACM rate parameters are similar to estimates from the Monte Carlo simulations. SOA gas-phase precursors in CACM present relative errors that range from 30% at a VOC:NO_x ratio of 8:1 to 39% when the ratio changes to 32:1. INDEX TERMS: 0305 Atmospheric Composition and Structure: Aerosols and particles (0345, 4801); 0317 Atmospheric Composition and Structure: Chemical kinetic and photochemical properties; 0345 Atmospheric Composition and Structure: Pollution—urban and regional (0305); KEYWORDS: tropospheric chemistry mechanism, secondary organic aerosol, Latin hypercube sampling, polluted urban areas, reaction rates

Citation: Rodriguez, M. A., and D. Dabdub, Monte Carlo uncertainty and sensitivity analysis of the CACM chemical mechanism, *J. Geophys. Res.*, 108(D15), 4443, doi:10.1029/2002JD003281, 2003.

1. Introduction

[2] The importance of air quality models (AQMs) resides partly in their ability to evaluate potential atmospheric responses that affect the concentration of key pollutants to different simulation conditions such as emissions control measures. A quantitative analysis of model responses provides valuable information to characterize sources of uncertainty. This type of analysis also serves to identify those parameters to which the model output is most sensitive. Emissions inventories represent the largest uncertainties associated with output concentrations in threedimensional urban/regional models [Griffin et al., 2002a]. However, the gas-phase chemical mechanism could introduce significant uncertainties in model predictions. Sources of uncertainty in chemical mechanisms lie in the rate constants, the product yields, and the mechanisms of degradation for generation products. Mathematical procedures to analyze uncertainty and sensitivity of complex photochemical mechanisms have been evaluated thoroughly. For instance, Dunker [1981, 1984], Milford et al. [1992], and Gao et al. [1995] used direct decoupled methods; Rabitz et al. [1983] and Rabitz and Hales [1995] employed the Green's Function or Adjoint Green's Function methods; whereas Carmichael et al. [1997] favored automatic differentiation techniques. Monte Carlo methods that examine uncertainties in chemical parameters have been applied also to gas-phase chemistry and photochemical box models [Stolarski et al., 1978; Ehhalt et al., 1979; Thompson and Stewart, 1991; Gao et al., 1995; Yang et al., 1996]. Monte Carlo methods are widely used because they can be applied to problems with a large number of input parameters. Furthermore, Monte Carlo methods also have the advantage that estimates of the uncertainties in model outputs are calculated with systematic runs of the model and that standard statistical tests can be applied to output results.

[3] This study presents results of the uncertainty and sensitivity analysis of the Caltech Atmospheric Chemistry Mechanism (CACM) [Griffin et al., 2002a, 2002b; Pun et al., 2002]. CACM includes state-of-the-art treatment of ozone formation, but more importantly, it is the first detailed atmospheric chemical mechanism directed toward explicit prediction of formation of the semivolatile products that have the potential to be constituents of secondary organic aerosol (SOA). Emphasis is placed on the characterization of uncertainties for product concentrations that could constitute SOA. A global sensitivity analysis of the chemical mechanism is performed using Monte Carlo techniques combined with Latin hypercube sampling to vary simultaneously all chemical parameters over their full ranges of uncertainty. Uncertainties in rate parameters are propagated through box model simulations with CACM for three summer cases. Cases cover a range of initial concentrations of reactive organic gases and nitrogen oxides that represent various episodes of high ozone levels in polluted urban areas. In addition to the estimated uncertainties of gas-phase SOA precursor concentrations, similar calculations are performed for O₃, HCHO, H₂O₂, and peroxyacetyl nitrate (PAN).

[4] Section 2 provides a complete description of the Monte Carlo techniques, the simulation conditions, and the uncertainty factors for the mechanism parameters used. Discussion of the results is presented in section 3. Finally, conclusions are provided in section 4.

2. Methodology

[5] In the following work, sensitivity and uncertainty analysis are accomplished using statistical methods to identify reaction parameters whose changes present the largest effect in both the concentration of selected key species and their associated errors. This section describes the statistical sampling used, the multiple regression approach to estimate sensitivity coefficients, and the corresponding uncertainty assessment under the simulation conditions established.

2.1. Latin Hypercube Sampling

- [6] A conventional approach to address uncertainty assessment is to apply Monte Carlo techniques. This particular methodology has been used extensively in regional-scale gas-phase mechanisms [Derwent and Hov, 1988; Gao et al., 1996; Phenix et al., 1998; Bergin et al., 1999; Grenfell et al., 1999; Hanna et al., 2001; Vuilleumier et al., 2001]. Monte Carlo analysis investigates the response of model output (species mixing ratio) when the input variables (reaction rates) are changed by repeated sampling from some assumed joint probability distribution. The probability distribution of the species mixing ratio along with its mean and other characteristics are obtained from the evaluation of model output for each sample. Monte Carlo analysis using random sampling yields reasonable estimates for the mixing ratios distribution if the sample size is large. However, using a large number of sampled cases is computationally expensive. An alternative approach, which yields more precise estimates, is the use of a constrained Monte Carlo sampling scheme. One such scheme is Latin hypercube sampling (LHS) [McCay et al., 1979], a stratified sampling technique compared extensively with other techniques [Iman and Helton, 1984], and that is proven to be more efficient than straight Monte Carlo sampling.
- [7] Latin hypercube sampling selects n different values from each of the N_p total number of parameters treated as random variables in the following manner. The range of each variable is divided into n non-overlapping intervals on the basis of equal probability. One value from each interval is selected at random with respect to the probability density in the interval. This value is randomly paired with the n values of the other N_p variables. Thus the nN_p -tuplets constructed in this manner form the Latin hypercube sample. It is convenient to think of this sample as an $n \times N_p$ input matrix where the lth row contains specific values of each of the N_p input variables used on

the lth run of the computer model. The proper size of an LHS sample is a compromise between the number of runs and the required accuracy. In this study, sample sizes ranging from 100 to 3880 runs are used to test the convergence of the means and the corresponding standard deviations of selected species. Results reported hereinafter are obtained with a sample size of 1150 computational runs of the box model. Even though the random variables are sampled independently and paired randomly, the sample correlation coefficient of any of the nN_p -tuplets is not zero due to sampling fluctuations. The input parameters in this study are treated as independent and the correlation coefficients for the samples used never exceed a value of 0.015.

2.2. Multiple Linear Regression

[8] Sensitivity of the model output to the input parameters is determined with multiple linear regression analysis techniques [*Derwent and Hov*, 1988; *Gao et al.*, 1996]. The regression model is based on the following relationship:

$$\frac{c_{ij}}{c_i^*} = \beta_{i0} + \sum_{l=1}^{N_p} \beta_{il} \ \epsilon_l \ k^*_l \quad i = 1, \dots, N \quad j = 1, \dots, n, \quad (1)$$

where c_i^* is the mixing ratio of species i from a simulation with nominal inputs, c_{ij} is the mixing ratio of species i in the simulation j, k_l^* is the nominal value of the input parameter l, ϵ_l is the multiplicative uncertainty factor associated to the input parameter l, β_{l0} is a constant from the regression, β_{il} is the regression coefficient for species i with respect to the input parameter l, N is the number of species of interest, n is the number of simulated runs, and N_p is the total number of parameters treated as random variables. Equation (1) can be rewritten as

$$\frac{c_{ij}}{c_i^*} = \beta_{i0} + \sum_{l=1}^{N_p} \hat{\beta_{il}} \ \epsilon_l \qquad i = 1, \dots, N \quad j = 1, \dots, n,$$
 (2)

where $\hat{\beta}_{il}$ is a normalized regression coefficient,

$$\beta_{il} = \frac{\hat{\beta_{il}}}{k^*}.\tag{3}$$

Note that for any species, the mixing ratio from a simulation with nominal inputs $c_i^*(t)$ and the mixing ratio of the simulation $c_{ij}(t)$ are functions of time, hence its ratio. The previous relationships could be used at each time step to estimate the corresponding regression coefficients that in turn would be time varying functions. However, this approach is computational expensive. A 12-hour time average value for the regression coefficient is chosen instead, i.e.,

$$\left\langle \frac{c_{ij}}{c_i^*} \right\rangle = \left\langle \beta_{i0} \right\rangle + \sum_{l=1}^{N_p} \left\langle \hat{\beta}_{il} \right\rangle \epsilon_l \quad i = 1, \dots, N \quad j = 1, \dots, n, \quad (4)$$

in which the angle brackets represent the averaged values in the chosen period of time. The uncertainty factors are assumed to be time independent; therefore, their values are not affected by the average.

Table 1. Initial Concentrations^a

CACM Species	Concentration, ppm
ALKH	0.0003
ALKL	0.1202
ALKM	0.0209
AROH	0.0183
AROL	0.0144
AROO	0.0002
BIOL	0.0001
BIOH	0.0001
ETHE	0.0334
ISOP	0.0004
OLEL	0.0278
OLEH	0.0007
PAH	0.0027
VOC species total, ppmC	1.5342
CH ₄	3.0
CO	3.2080
CO_2	0.0170
HONO	0.0020
HNO ₃	0.0007
H_2O^b	15500.0
NO	0.0967
NO_2	0.0820
NH_3	0.0062
SO_2	0.0032

^aThe table lists initial conditions for a typical urban location such as Riverside, California, with a VOC/NO_x ratio of 8.6. For the examined urban cases, NO_x concentrations are adjusted to yield initial VOC/NO_x ratios of 8:1, 17:1 and 32:1.

^bEquivalent to a RH = 49.6% at atmospheric conditions considered in this study (P = 1 atm, T = 298°K).

[9] The contribution of each parameter to uncertainties in output concentrations is obtained from the propagation of error formula. However, to be consistent with the calculation of the regression coefficients, a time average contribution to uncertainty is defined as

$$u_{li} = \frac{\left(\sigma_l/k_l^*\right)^2 \left\langle \hat{\beta_{il}} \right\rangle^2}{\sum_{l=1}^{N_p} \left(\sigma_l/k_l^*\right)^2 \left\langle \hat{\beta_{il}} \right\rangle^2} \times 100, \tag{5}$$

in which the uncertainty contribution u_{li} of parameter l to the uncertainty of species i, depends on the nominal value of the input parameters k_l^* , the variance of each rate parameter σ_l , and the time-averaged regression coefficients $\hat{\beta}_{il}$. Equation (5) represents the average relative error associated with the reaction rate parameters (σ_l/k_l^*) divided by the total relative uncertainty of species i, and weighted by the estimated coefficients of the regression.

2.3. Simulation Conditions

[10] Computational runs performed in a box model with CACM as the chemical mechanism are the starting point for the proposed Monte Carlo analysis. The box model includes time-varying photolysis rates at a latitude of 34°N, approximately that of the Los Angeles basin. A 12-hour period that spans from 0600 to 1800 LT is chosen to study an episode where photolysis plays a major role in the formation of important species such as ozone. Initial conditions used represent those of an urban environment. Initial conditions for all species are obtained from typical data provided by the three-dimensional CIT model [Harley et al., 1993; Meng et al., 1998]. The cell selected from the CIT

model represents Riverside because this location exhibits large ozone concentrations in the Southern California Basin. Typical VOC to NO_x ratios in urban regions vary from 6:1 to 50:1 [Baugues, 1986]. Urban summer surface conditions [Gao et al., 1995] range from 6:1 to 24:1 with 1000 ppbC total VOC mixing ratio. The value of the initial VOC/NO_x ratio in the chosen cell is 8.6 with 1534 ppbC total VOC. However, different cases for the VOC/NO_x ratio are analyzed by changing the NO_x mixing ratio. Three cases are examined. First, the ratio is set at 8:1, corresponding to regions in which ozone increases as NO_x gets reduced. Second, the optimal ratio for maximum ozone production is set at 17:1. Finally, a ratio of 32:1 corresponds to the region where decreasing NO_x results in further O₃ reduction. Details on the initial concentrations used in this study are shown in Table 1. Also, a subset of the terms used to represent the different chemical species in CACM is provided in Table 2.

[11] All rate parameters are treated as random variables. Uncertainty estimates for the kinetic parameters of CACM are compiled mostly from published reviews [DeMore et al., 1990; Gao et al., 1996], and from the Summary of Evaluated Kinetic and Photochemical Data for Atmospheric Chemistry (available from Atkinson et al. at the World Wide Web server for the IUPAC Subcommittee for Gas

Table 2. Subset of Chemical Species in CACM^a

	1	
Term	Description	
ALD2	lumped higher aldehydes (<i>n</i> -pentanal)	
ALKL	lumped alkanes C_2 – C_6 (2-methyl-butane)	
ALKM	lumped alkanes $C_7 - C_{12}$ (3,5-dimethyl-heptane)	
ALKH	lumped alkanes $> C_{12}$ (<i>n</i> -hexadecane)	
AROL	lumped low SOA yield aromatic	
	species (1,2,3-trimethyl-benzene)	
AROH	lumped high SOA yield aromatic	
	species (3- <i>n</i> -propyl-toluene)	
AROO	lumped phenolic species (2,6-dimethyl-phenol)	
ARAL	lumped aromatic monoaldehydes (p-tolualdehyde)	
BIOL	lumped low SOA yield monoterpene	
	species (α -terpineol)	
BIOH	lumped high SOA yield monoterpene	
	species (γ-terpinene)	
KETL	lumped ketones C_3-C_6 (2-pentanone)	
KETH	lumped ketones $> C_6$ (2-heptanone)	
ISOP	isoprene	
MGLY	methyl glyoxal	
MVK	methyl-vinyl-ketone	
ETHE	ethene	
OLEL	lumped alkenes C_2-C_6 (1-pentene)	
OLEH	lumped alkenes $> C_6$ (4-methyl-1-octene)	
OSD	$O(^{1}D)$	
PAH		
	aromatic hydrocarbons	
	(1,2-dimethyl-naphthalene)	
PAN1	peroxy pentionyl nitrate	
PAN2	peroxy acetyl nitrate (PAN)	
RAD_3	hexadienyl radical from OH oxidation of AROL	
RAD_4	hexadienyl radical from OH oxidation of AROH	
RO_26	acyl radical from aldehydic H abstraction of ALD2	
RO_28	acyl peroxy radical <c<sub>6 from</c<sub>	
	oxidation of ALD2, ISOP, BIOH,	
	MVK, KETL, KETH and BIOL (C_2)	
RO_234	peroxy radical from addition of O ₂ to RAD ₃	
RO_235	peroxy radical from addition of O ₂ to RAD ₄	
RP11	4, 5-dimethyl-6-keto-2, 4-heptadienal	
RP15	2-formyl-acetophenone	

^aA complete description of all terms used to represent chemical species in CACM is presented by *Griffin et al.* [2002a].

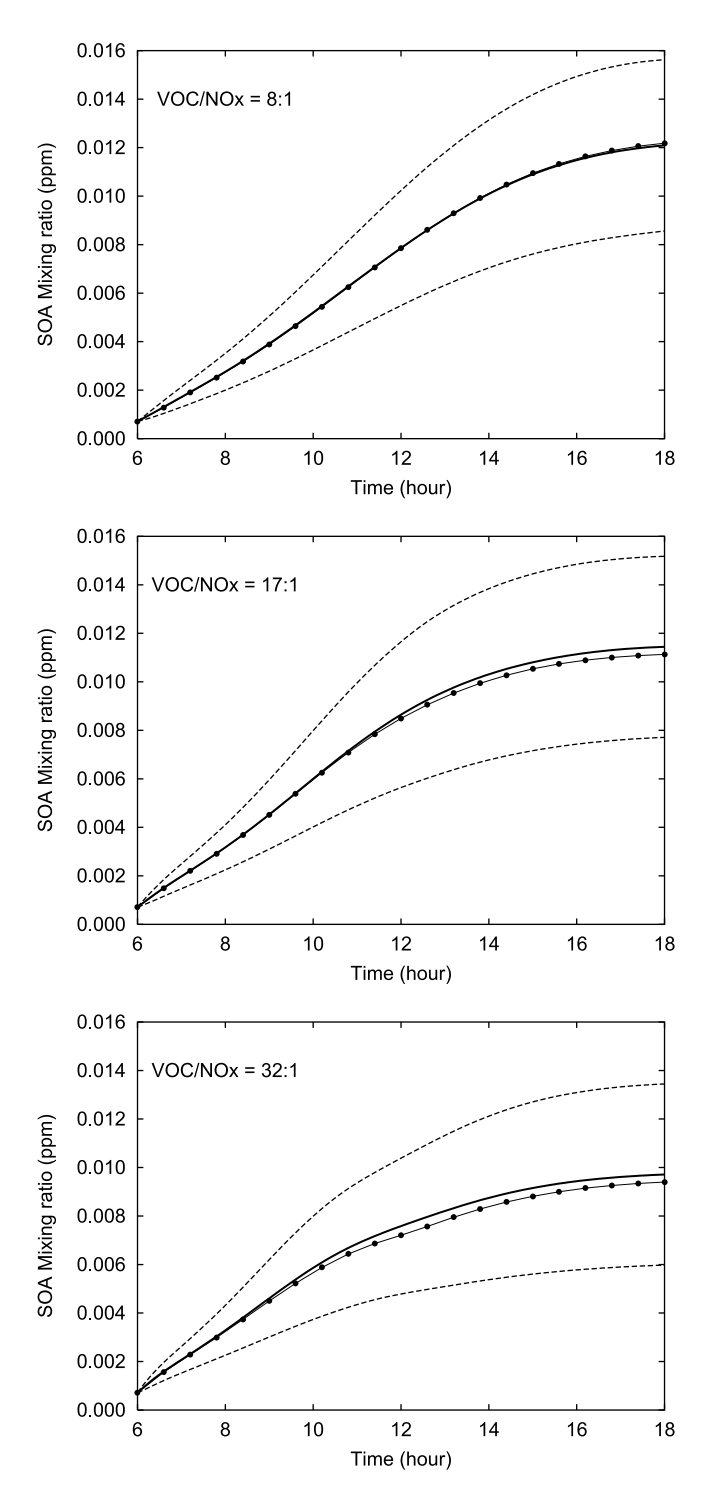


Figure 1. Mean concentrations and 1σ uncertainty ranges for gas-phase SOA precursors at different VOC/NO_x ratios. Solid line, mean from all results; line with circles, concentrations with nominal parameters; dashed curves, 1σ uncertainty bounds for results.

Kinetic Data Evaluation, http://www.iupac-kinetic.ch.cam.ac.uk/index.html).

3. Results

[12] This section focuses in the systematic examination of those chemical mechanism features to which prediction of semi-volatile products and ozone formation is more sensitive. In addition, this section presents a similar analysis for rate parameters of reactions associated to selected species in the model.

3.1. Uncertainty Analysis of SOA Precursors

[13] A major objective in the formulation of CACM is the prediction of concentrations related to surrogate organic products with the potential to partition into the aerosol phase. Griffin et al. [2002a] detailed the criteria followed to identify those products considered to have the potential to partition into the aerosol phase. The same products are selected to represent the potential SOA components and are referred to as SOA precursors hereinafter. Figure 1 shows the mean concentrations of SOA gas-phase precursors and their corresponding 1_{\sigma} uncertainty bounds at different VOC/NO_x. SOA precursor concentrations predicted using nominal rate parameters are close to mean values (best estimates) from the Monte Carlo simulations. For instance, the largest root mean square (RMS) value (0.0003) occurs at a VOC/NO_x ratio of 32:1. Results with nominal values are indistinguishable from those obtained with the best estimates at a VOC/NO_x ratio of 8:1 (RMS = 4.3×10^{-5}), whereas at larger ratios there is a small underprediction after 6 hours of simulation. However, nominal values still fall well within 1 standard deviation from the mean. After simulating 12 hours, SOA precursor concentrations range from 10 ± 4 ppb at a VOC/NO_x ratio of 32:1 to 12 ± 4 ppb at a VOC/NO_x ratio of 8:1. Relative uncertainties are calculated for SOA precursors as the ratio of the estimated standard deviation (σ) to the mean concentration values. In general, these relative uncertainties are not constant during the interval studied. Figure 2 shows the relative uncertainties of SOA precursors as a function of time for all the different VOC/NO_x ratios considered. Relative errors of SOA precursors in CACM show a similar behavior for all cases analyzed. Errors increase during the morning but then remain fairly constant throughout the rest of the day. Figure 2 also shows that the chemical mechanism consistently exhibits larger errors when the VOC/NO_x ratio increases.

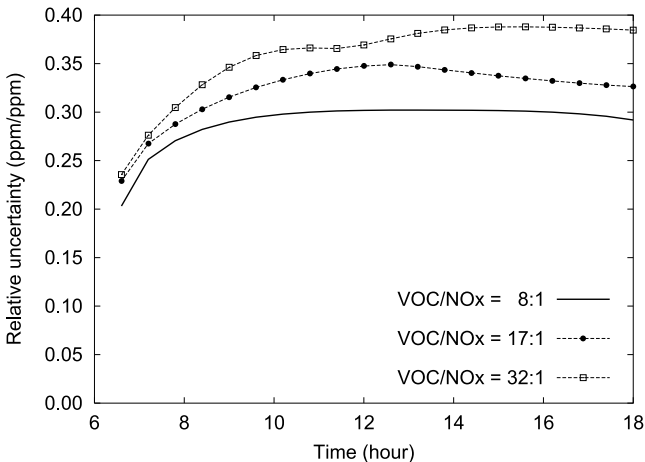


Figure 2. Relative uncertainty for gas-phase SOA precursor concentrations as a function of time for indicated VOC/NO_x ratios. Uncertainty is defined as the estimated σ divided by the mean from all results.

Table 3. Summary of Relative Uncertainties for 12-hour Average Monte Carlo Results of Selected Product Species^a

,	VOC/NO _v	-	R	elative Unc	ertainty, %	b	
	Ratio	O_3	НСНО	H_2O_2	HNO_3	PAN	SOA
	8:1	44(18:00)	22(16:12)	163(18:00)	21(13:48)	73(11:42)	30(12:48)
	17:1	28(10:36)	25(17:36)	184(12:00)	21(10:12)	59(9:12)	35(12:30)
	32:1	26(8:42)	28(17:12)	154(9:24)	19(8:42)	55(8:42)	39(15:24)

^aValues in parentheses show the time in which the maximum relative uncertainty in a 12-hour period occurs.

- [14] Reducing the information from these plots to a single value to represent the uncertainty at all times could lead to misleading conclusions. For instance, the final relative error might not represent properly the uncertainty associated to predicted concentrations with the chemical mechanism. Since one goal of this analysis is to place general error bounds for the species considered, absolute maxima calculated from plots in Figure 2 are chosen as maxima relative errors for predicted SOA precursors concentrations. This, in effect, places the largest possible error bounds for the species concentrations calculated with CACM. Note that the time at which each maximum occurs is not necessarily the same for all the cases analyzed. Table 3 summarizes the maximum relative uncertainty and the time at which the maximum occurs for selected species in the 12-hour period used. The maximum relative error shown by SOA gas-phase precursors in CACM is 30% at a VOC/NO_x ratio of 8:1 and 35% at a 17:1 ratio, whereas the largest maximum error (39%) is placed at the 32:1 ratio.
- [15] Multiple linear regression is used to investigate the most sensitive reactions of key species. The uncertainty analysis methodology described above recognizes the reactions that are major contributors to the species total error. In the case of SOA gas-phase precursors, this approach explains and identifies the different contributions to the total uncertainty as reflected on the R^2 values that range from 0.90 to 0.95 for the different VOC/NO_x ratios studied. R^2 values suggest that the results obtained using a linear regression model are reliable. Moreover, good agreement exists between predicted concentrations by the linear regression and those obtained from the Monte Carlo simulations as illustrated in Figure 3. This figure shows scatterplots for the average ratio of predicted versus simulated SOA precursor concentrations to nominal SOA concentrations at different VOC/NO_x ratios.
- [16] Table 4 presents the most important reactions in the formation of SOA precursors, ordered by the percentage in which they contribute to the estimated relative uncertainty. This table also reports normalized regression coefficients. The absolute value of the regression coefficients represents a measure of the sensitivity of SOA gas-phase precursors to changes in the reaction rates. Table 4 provides information to distinguish those reactions whose contribution to the total uncertainty have a considerable effect on the production or loss of SOA precursors. Major contributors to the uncertainty of SOA predictions are the NO₂ and HCHO photolysis, and the reaction of lumped low SOA yield aromatic species with OH at VOC/NO_x ratios less than 17:1. At higher ratios, NO₂ photolysis still contributes the most to

the uncertainty, but reaction of cyclohexadienyl peroxy radical (RO₂34) with NO is now also important. Regression analysis shows that at VOC/NO_x ratios less than 17:1, SOA gas-phase precursor concentrations are more sensitive to

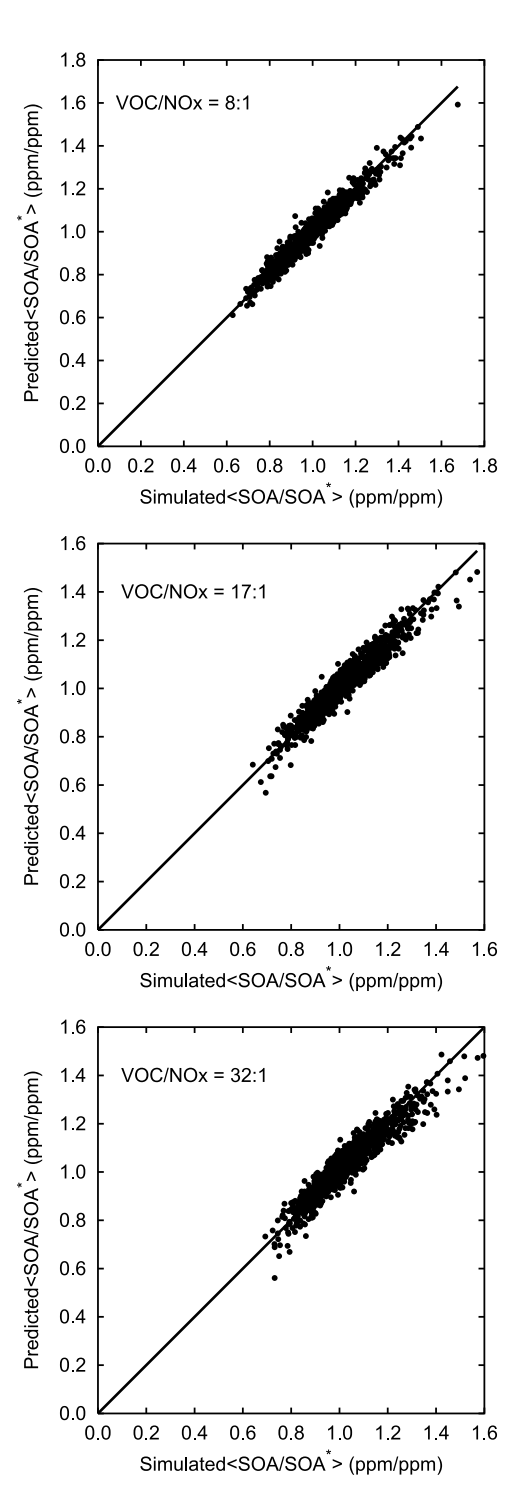


Figure 3. Predicted versus simulated average gas-phase SOA precursor concentrations to nominal precursor concentrations (SOA*) ratio at different VOC/NO_x ratios. Line shows the one to one correspondence. Simulated values are obtained from the Monte Carlo simulations, whereas predicted values represent the best possible estimates from the multiple linear regression model.

^bRelative uncertainty (%) = $100 \times \max(\sigma/\mu)$ in 12-hour simulation period.

Table 4. Most Important Parameters Based on the Contributions to Uncertainty on the Time-Averaged of Gas-Phase SOA Precursors Concentrations

Reaction:Product	Regression Coefficient	Uncertainty Contribution, %			
$VOC/NO_x = 8:1, R^2 = 0.95$					
$VOC/NO_x = 8:1, R = 0.95$ HCHO + $h\nu \to CO + 2 HO_2$ 0.173 21					
AROL + OH	0.169	12			
$NO_2 + h\nu$	0.141	9			
$NO_2 + OH + M$	-0.376	8			
AROH + OH	0.134	8			
PAH + OH	0.076	6			
$ALD2 + h\nu$	0.082	5			
$MGLY + h\nu$	0.053	4			
RP11 + OH	0.061	4			
$NO + O_3$	-0.167	2			
RO ₂ 34	-0.033	2			
RO ₂ 35	-0.020	1			
RP15 + OH	0.010	0.1			
ARAL + OH	0.010	0.1			
$VOC/NO_x =$	$= 17:1, R^2 = 0.93$				
$NO_2 + h\nu$	0.168	13			
AROL + OH	0.148	10			
$\mathrm{HCHO} + h\nu \rightarrow \mathrm{CO} + 2 \; \mathrm{HO}_2$	0.110	9			
RO_234	-0.061	8			
AROH + OH	0.127	7			
$RO_234 + NO$	0.059	7			
$RO_235 + NO$	0.049	5			
$MGLY + h\nu$	0.054	5			
PAH + OH	0.059	4			
RO ₂ 35	-0.040	3			
$NO + O_3$	-0.182	2			
RP15 + OH ARAL + OH	0.027	1 0.3			
ARAL + OH	0.016	0.3			
$VOC/NO_x =$	$= 32:1, R^2 = 0.90$				
$NO_2 + h\nu$	0.184	15			
$RO_234 + NO$	0.068	9			
RO_234	-0.065	8			
AROL + OH	0.134	8			
ALD2 + OH	-0.114	6			
AROH + OH	0.113	6			
$HCHO + h\nu \rightarrow CO + 2 HO_2$	0.085	5 5 3			
$RO_235 + NO$	0.051	5			
PAH + OH	0.054	3			
RO ₂ 35	-0.040	3			
RP15 + OH	0.052	3 2			
$NO + O_3$	-0.189	1			
ARAL + OH	0.026	1			

OH loss by reaction with NO2. This suggests that OH oxidation of reactive organic gases is the most predominant pathway for SOA precursors formation. At the lowest ratio analyzed, this pathway is even more important as HO₂ formation by formaldehyde photolysis becomes the second most important rate parameter. However, at the 17:1 ratio, oxidation by ozone starts to become significant as the second and third more sensitive reactions are the O₃ loss with NO and O₃ gain due to NO₂ photolysis, respectively. In fact, the sensitivity of SOA precursors to the reaction of O₃ with NO becomes even more relevant at the 32:1 VOC/NO_x ratio. Griffin et al. [2002a] indicated that aromatics are an important anthropogenic source of SOA and that sensitivity of SOA predicted from aromatic precursors to key aspects of aromatic photooxidation merits evaluation. These authors looked into the isomerization of radicals formed in aromatic-OH chemistry and found that halving this rate constant results in a significant increase in the amount of organic

mass with the potential to form SOA. The current analysis shows that these reactions are not the most influential in the formation of SOA; however, the negative value of their regression coefficients is consistent with *Griffin et al.* [2002a] in that a reduction in the rate parameters would result in increasing the concentration of SOA precursors.

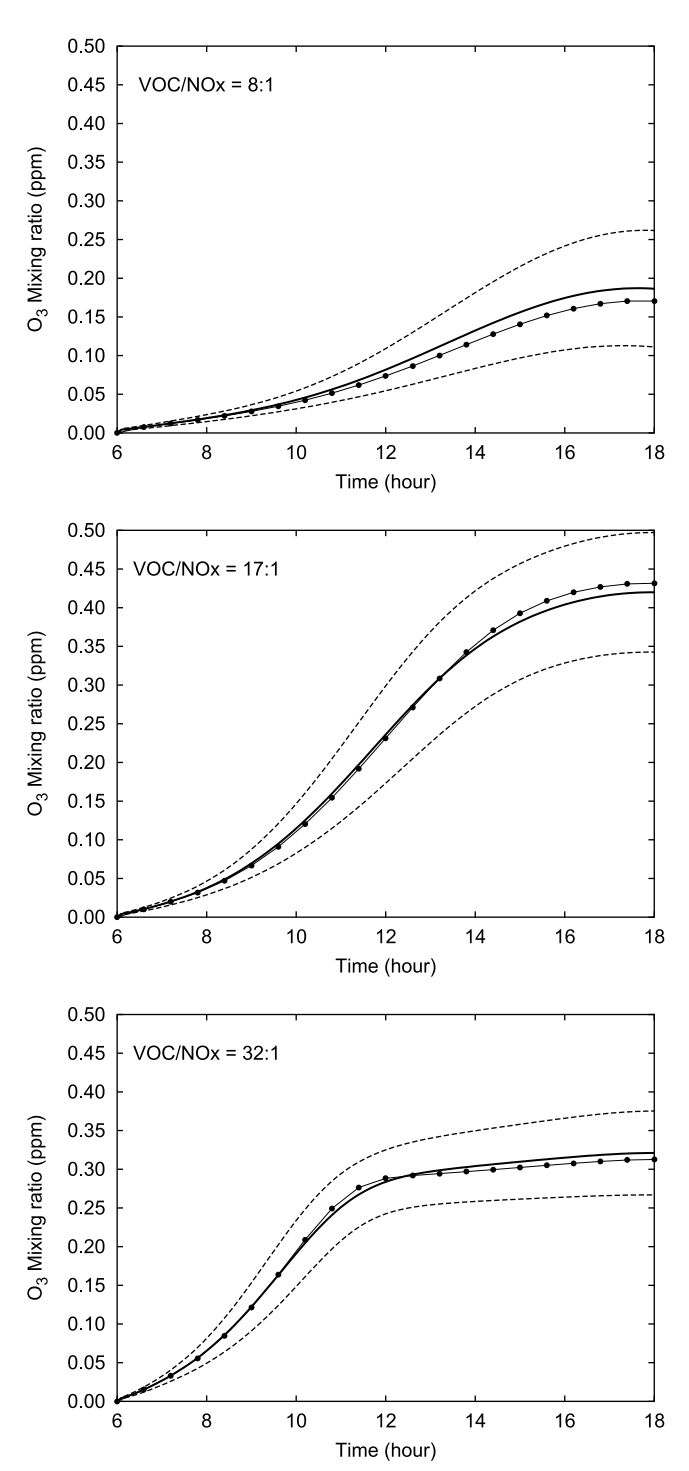


Figure 4. Mean concentrations and 1σ uncertainty ranges for ozone at different VOC/NO_x ratios. Solid line, mean from all results; line with circles, concentrations with nominal parameters; dashed curves, 1σ uncertainty bounds for results.

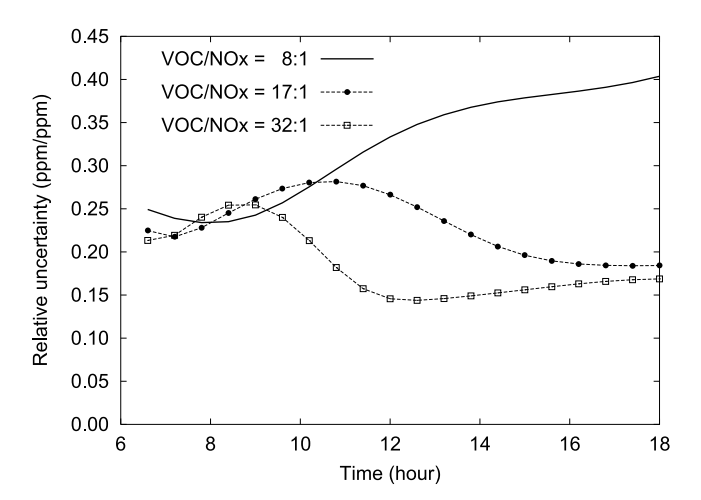


Figure 5. Relative uncertainty for ozone as a function of time for indicated VOC/NO_x ratios. Uncertainty is defined as the estimated σ divided by the mean from all results.

Furthermore, in terms of the most influential reactions involving aromatics, the most sensitive reactions are those associated with the bridging reaction of peroxy radicals (RO₂34 and RO₂35) from addition of O₂ to radicals produced by OH oxidation of both lumped low and high SOA yield aromatic species, respectively. *Griffin et al.* [2002a] also examined the direct conversion of aldehydes to semivolatile organic acids. They discovered that total SOA material decreases when the acid formation yield is halved. The present study agrees with this finding, in addition, this work shows that from the reactions involving aldehydes conversion, the greatest effect on SOA occurs with OH oxidation of 2-formyl-acetophenone (RP15) and the lumped aromatic monoaldehydes (ARAL).

3.2. Uncertainty Analysis of O₃

[17] Figure 4 shows mean ozone concentrations and their corresponding 1_{\sigma} uncertainty bounds as a function of time for each simulated case. Final ozone concentrations range from 186 \pm 75 ppb at a VOC/NO_x ratio of 8:1 to 420 \pm 77 ppb at a VOC/NO_x ratio of 17:1. At VOC/NO_x ratios higher than 17:1, O₃ concentrations using nominal CACM parameters are closer to the mean values from the Monte Carlo simulations (RMS = 0.007 at 17:1 ratio, RMS = 0.006at 32:1 ratio). At the 8:1 ratio, the nominal parameters lead to concentrations that are consistently underpredicted compared to the best estimates (RMS = 0.01); however, they still lie within 1 standard deviation. Figure 5 shows the time variation for ozone relative uncertainties. This figure illustrates that CACM exhibits the largest relative errors for ozone concentrations at a VOC/NO_x ratio of 8:1 where the maximum error is 44%, these uncertainties then decrease at the 17:1 ratio (28%), and are the smallest at 32:1 (down to 26%).

[18] Figure 6 shows scatterplots of the average ratio of predicted versus simulated ozone concentrations to the calculated values with nominal parameters at different VOC/NO_x ratios. There exists good agreement between predicted values by the linear regression model and those obtained from the Monte Carlo simulation for all different ratios analyzed. Table 5 shows the most important reactions

ordered in terms of their contribution to ozone relative uncertainty from most to less uncertain. Regression analysis shows that at VOC/NO_x ratios less than 17:1, the NO₂ photolysis rate and HCHO + $h\nu \rightarrow$ CO + 2 HO₂ are the

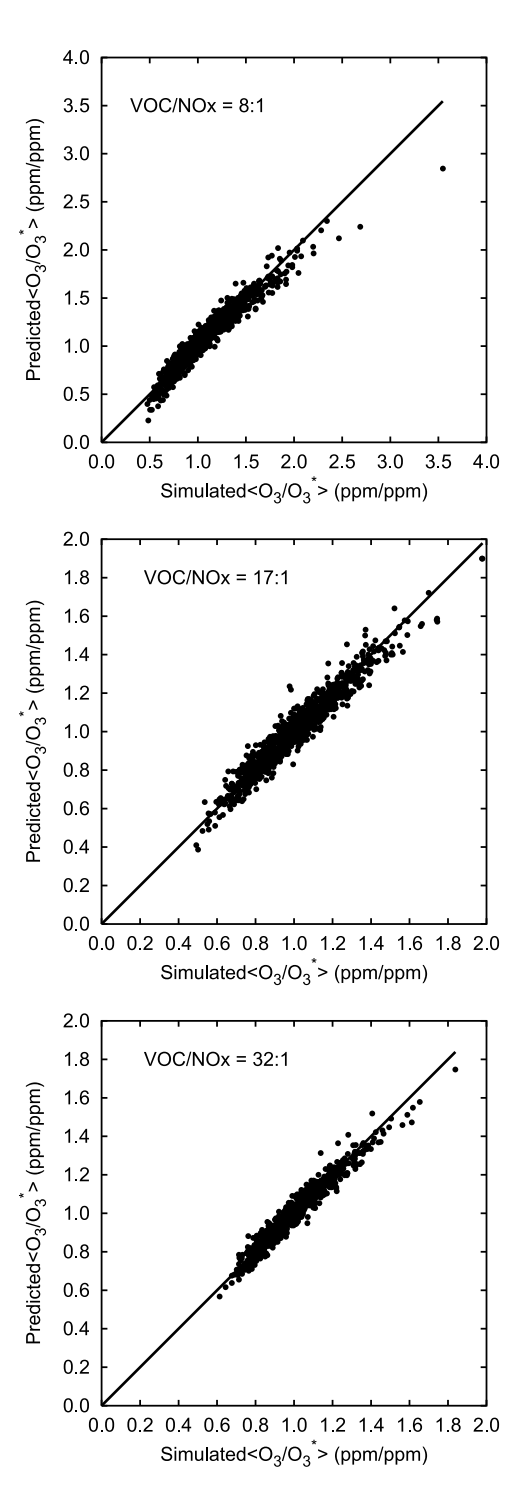


Figure 6. Predicted versus simulated average ozone (O_3) to nominal ozone concentration (O_3^*) ratio at different VOC/NO_x ratios. Line shows the one to one correspondence. Simulated values are obtained from the Monte Carlo simulations, whereas predicted values represent the best possible estimates from the multiple linear regression model.

Table 5. Most Important Parameters Based on the Contributions to Uncertainty on the Time-Averaged O₃ Concentrations

	Regression	Uncertainty				
Reaction:Product	Coefficient	Contribution, %				
$VOC/NO_x = 8:1, R^2 = 0.94$						
$HCHO + h\nu \rightarrow CO + 2 HO_2$	0.413	25				
$NO_2 + h\nu$	0.470	19				
$ALD2 + h\nu$	0.240	8				
$NO_2 + OH + M$	-0.699	5				
$MGLY + h\nu$	0.127	5				
$NO + O_3$	-0.591	4				
$RO_234 + NO$	-0.088	3				
ALKL + OH	0.181	3				
RO ₂ 34	0.080	2				
HCHO + $h\nu$	-0.125	2				
$VOC/NO_x = 17:1, R^2 = 0.94$						
$NO_2 + h\nu$	0.341	21				
$HCHO + h\nu \rightarrow CO + 2 HO_2$	0.220	15				
$MGLY + h\nu$	0.142	12				
$RO_26 + NO$	0.085	6				
$RO_2^26 + NO_2 + M$	-0.106	3				
$RO_234 + NO$	-0.064	3				
$NO + O_3$	-0.364	3				
$ALD2 + h\nu$	0.097	3				
RO ₂ 34	0.055	2				
$NO_2 + OH + M$	-0.319	2				
$VOC/NO_x = 32:1, R^2 = 0.95$						
$NO_2 + h\nu$	0.342	35				
$RO_2^-6 + NO$	0.091	11				
$MGLY + h\nu$	0.085	7				
$RO_26 + NO_2 + M$	-0.110	6				
PAN1	0.094	4				
$RO_28 + NO$	0.057	4				
$HCHO + h\nu \rightarrow CO + 2 HO_2$	0.088	4				
$NO + O_3$	-0.306	4				
PAN2	0.082	3				
$RO_28 + NO_2 + M$	-0.080	3				

most uncertain reaction rates. However, ozone is most sensitive to changes in the reaction rate of O₃ with NO to regenerate NO₂ and the reaction of OH with NO₂ to produce nitric acid. Reactions that also contribute to the total uncertainty of ozone are methyl glyoxal (MGLY) and the lumped higher aldehydes photolysis. This is consistent with the original formulation of CACM, since MGLY is modeled to behave as an aldehyde. Results at VOC/NO_x ratios of 32:1 differ from those at lower ratios. Although NO₂ photolysis still shows that it is the major contribution to ozone uncertainty, the second most uncertain rate parameter is that of the reaction of the acyl radical (RO₂6) from aldehydic H abstraction of the lumped aldehydes with NO. However, in terms of sensitivity, ozone loss with NO is more important than that of RO₂6. The fact that reactions that involve the acyl radical RO₂6, the acyl peroxy radical RO₂8, and peroxy alkyl nitrates (PAN1 and PAN2) become relevant at these ratios is a consequence of the low NO_x concentrations; therefore peroxy radical reactions begin to become important. At sufficiently low NO_x concentrations or high VOC/NO_x ratios, a further decrease in NO_x favors peroxy-peroxy reactions that in effect retard O₃ formation by removing free radicals from the system.

3.3. Uncertainty Analysis of Selected Species

[19] Table 3 summarizes the maximum relative uncertainty for selected key species in the 12-hour period.

Hydrogen peroxide concentrations present the highest uncertainties (±184% in the 17:1 case); however, these values are associated with mean H₂O₂ concentrations that are very low (no larger than 6 ppb for the 17:1 case). Relative uncertainties for PAN range from ±55% to 73%, for formaldehyde between ±22% to 28%, whereas for nitric acid range from $\pm 19\%$ to 21%. Overall, the largest uncertainties in CACM correspond to PAN and H₂O₂, while the lowest uncertainties are exhibited by HNO₃ and HCHO. Uncertainties for O₃ and the total gas-phase SOA precursors fall between these two bounds. Multiple linear regression is used to identify the most sensitive reactions to selected species (Table 6) as well as the major contributors to the total uncertainty displayed by CACM. In general, this approach explains and identifies different contributions to the total uncertainty as reflected

Table 6. Most Important Parameters Based on the Contributions to Uncertainty on the Time-Averaged Concentrations of Key Species in Selected Cases

species in Selected Cases						
	Regression	Uncertainty				
Reaction:Product	Coefficient	Contribution, %				
HNO3: VOC/NO	$x = 8:1, R^2 = 0.95$					
$HCHO + h\nu \rightarrow CO + 2 HO_2$	0.254	32				
$NO_2 + H_2O$	0.221	14				
$ALD2 + h\nu$	0.128	8				
$MGLY + h\nu$	0.089	8				
$RO_234 + NO$	-0.053	4				
RO ₂ 34	0.049	3				
$O_3 + h\nu \rightarrow OSD + O_2$	0.098	3				
HCHO + $h\nu$	-0.068	2				
$HNO_3 + OH$	-0.086	2				
$RO_235 + NO$	-0.041	2				
PAN: $VOC/NO_x = 8:1$, $R^2 = 0.83$						
$RO_28 + NO$	-0.537	20				
PAN2	-0.758	15				
$RO_28 + NO_2 + M$	0.697	13				
$HCHO + h\nu \rightarrow CO + 2 HO_2$	0.528	7				
$MGLY + h\nu$	0.317	5				
$ALD2 + h\nu$	0.428	5				
RO ₂ 34	0.211	3				
$NO_2 + OH + M$	-0.968	2				
$NO_2 + h\nu$	-0.348	2				
RO_2 34 + NO	-0.161	2				
- HCHO, VOCING	$Q_x = 8:1, R^2 = 0.95$					
HCHO: VOC/NO HCHO + $h\nu \rightarrow \text{CO} + \text{H}_2$	-0.330	63				
$HCHO + h\nu \rightarrow CO + H_2$ $HCHO + h\nu \rightarrow CO + 2 HO_2$	-0.330 -0.095	5				
$MGLY + h\nu \rightarrow CO + 2 HO_2$	0.049	3				
OLEL + OH		3				
	0.191 -0.099	2				
HCHO + OH		2				
RO ₂ 34 + NO	-0.035	2				
$NO_2 + OH + M$ $ALD2 + h\nu$	-0.203 0.055	2				
		2				
RO ₂ 34 RO ₂ 35 + NO	$0.032 \\ -0.032$	2				
KO ₂ 33 + NO	-0.032	2				
H_2O_2 : $VOC/NO_x = 32:1$, $R^2 = 0.49$						
$HCHO + h\nu \rightarrow CO + 2 HO_2$	0.412	15				
$ALD2 + h\nu$	0.297	8				
$O_3 + h\nu \rightarrow OSD + O_2$	0.241	3				
$NO_2 + OH + M$	-0.665	3 3				
$OSD + H_2O$	0.318	3				
OSD + M	-0.305	2 2 2 2				
$HCHO + h\nu \rightarrow CO + H_2$	-0.156	2				
$HNO_3 + OH$	-0.201	2				
$RO_234 + NO$	-0.094					
$RO_28 + NO$	0.092	2				

on the \mathbb{R}^2 values that range from 0.83 to 0.95 for most key species.

4. Conclusions

- [20] Monte Carlo techniques combined with Latin hypercube sampling are used to perform more than 3000 runs in order to present the first detailed uncertainty and sensitivity analysis of the CACM chemical mechanism. Results suggest that SOA gas-phase precursors in CACM exhibit maximum relative errors that range from 30% at a VOC/NO_x ratio of 8:1, to 39% when the ratio changes to 32:1. This study confirms some of the findings presented by other authors. Although the current analysis shows that reactions involving aromatics photooxidation and the direct conversion of aldehydes to semivolatile organic acids are not the most influential in SOA formation, the effects of changing the reaction rate parameters agree well with previous findings [Griffin et al., 2002a]. Results for selected key species (HNO₃, PAN, HCHO, H₂O₂) reproduce similar features as those exposed by other researchers [Gao et al., 1996].
- [21] This work also presents new findings about the dynamics of SOA precursors. Namely, major contributors to the uncertainty of SOA predictions are the NO₂ and HCHO photolysis, and the reaction of lumped low SOA yield aromatic species with OH at VOC/NO_x ratios less than 17:1. This study also finds that SOA precursor concentrations are most sensitive to OH loss by the reaction with NO₂ at low VOC/NO_x ratios. However, at higher ratios, O₃ oxidation with NO becomes one of the most relevant reactions affecting the formation of SOA.
- [22] Acknowledgments. This study has been supported by the UC-Mexus Scholarship and the CAREER Award grant ATM-9985025 from the National Science Foundation. Any opinions, findings, and conclusions or recommendations expressed in this material are those of the authors and do not necessarily reflect the views of the National Science Foundation. The authors are grateful to Robert Griffin for his thorough review of this paper. We are also thankful to Scott Samuelsen and Jack Brower from the Advanced Power and Energy Program for their comments and constructive criticism.

References

- Baugues, K., A review of NMOC, NO_x ratios measured in 1984 and 1985, *Rep. EPA/450/4-86-015*, U.S. Environ. Prot. Agency, Research Triangle Park, N. C., 1986.
- Bergin, M. S., G. S. Noblet, K. Petrini, J. R. Dhieux, J. B. Milford, and R. A. Harley, Formal uncertainty analysis of a Lagrangian photochemical air pollution model, *Environ. Sci. Technol.*, 33, 1116–1126, 1999.
- Carmichael, G. R., A. Sandu, and F. A. Potra, Sensitivity analysis for atmospheric chemistry models via automatic differentiation, *Atmos. Environ.*, 31, 475–489, 1997.
- DeMore, W. B., S. P. Sander, D. M. Golden, M. J. Molina, R. F. Hampson, M. J. Kurlyo, C. J. Howard, and A. R. Ravishankara, Chemical kinetics and photochemical data for use in stratospheric modeling, evaluation number 9, JPL Publ., 90-1, 1990.
- Derwent, R., and O. Hov, Application of sensitivity and uncertainty analysis techniques to a photochemical ozone model, *J. Geophys. Res.*, 93, 5185–5199, 1988.
- Dunker, A. M., Efficient calculation of sensitivity coefficients for complex atmospheric models, Atmos. Environ., 15, 1155–1161, 1981.
- Dunker, A. M., The decoupled direct method for calculating sensitivity coefficients in chemical kinetics, J. Chem. Phys., 81, 2385-2393, 1984.

- Ehhalt, D. H., J. S. Chang, and D. M. Butler, The probability distribution of the predicted CFM-induced ozone depletion, *J. Geophys. Res.*, 84, 7889–7894, 1979.
- Gao, D., W. R. Stockwell, and J. B. Milford, First-order sensitivity and uncertainty analysis for a regional-scale gas-phase chemical mechanism, *J. Geophys. Res.*, 100, 23,153–23,166, 1995.
- Gao, D., W. R. Stockwell, and J. B. Milford, Global uncertainty analysis of a regional-scale gas-phase chemical mechanism, *J. Geophys. Res.*, 101, 9107–9119, 1996.
- Grenfell, J. L., et al., Tropospheric box-modelling and analytical studies of the hydroxyl (OH) radical and related species: Comparison with observations, *J. Atmos. Chem.*, *33*, 183–214, 1999.
- Griffin, R. J., D. Dabdub, and J. H. Seinfeld, Secondary organic aerosol: 1. Atmospheric chemical mechanism for production of molecular constituents, *J. Geophys. Res.*, 107(D17), 4332, doi:10.1029/2001JD000541, 2002a.
- Griffin, R. J., D. Dabdub, M. J. Kleeman, M. P. Fraser, G. R. Cass, and J. H. Seinfeld, Secondary organic aerosol: 3. Urban/regional scale model of size- and composition-resolved aerosols, *J. Geophys. Res.*, 107(D17), 4334, doi:10.1029/2001JD000544, 2002b.
- Hanna, S. R., Z. G. Lu, H. C. Frey, N. Wheeler, J. Vukovich, S. Arunachalam, M. Fernau, and D. A. Hansen, Uncertainties in predicted ozone concentrations due to input uncertainties for the UAM-V photochemical grid model applied to the July 1995 OTAG domain, *Atmos. Environ.*, 35, 891–903, 2001.
- Harley, R. A., A. G. Russell, G. J. McRae, G. R. Cass, and J. H. Seinfeld, Photochemical modeling of the Southern California Air Quality Study, Environ. Sci. Technol., 26, 2395–2408, 1993.
- Iman, R. L., and J. C. Helton, A comparison of uncertainty and sensitivity techniques for computer models, *Rep. SAND83-2365*, U.S. Dep. of Energy, Sandia Natl. Lab., Albuquerque, N. M., 1984.
- McCay, M. D., W. J. Conover, and R. J. Beckman, A comparison of three methods for selecting values of input variables in the analysis of output from a computer code, *Technometrics*, 221, 239–245, 1979.
- Meng, Z., D. Dabdub, and J. H. Seinfeld, Size-resolved and chemically resolved model of atmospheric aerosol dynamics, *J. Geophys. Res.*, 103, 3419–3435, 1998.
- Milford, J. D., D. Gao, A. G. Russell, and G. J. McRae, Use of sensitivity analysis to compare chemical mechanisms for air-quality modeling, *Environ. Sci. Technol.*, 26, 1179–1189, 1992.
- Phenix, B. D., J. L. Dinaro, M. A. Tatang, J. W. Tester, J. B. Howard, and G. J. McRae, Incorporation of parametric uncertainty into complex kinetic mechanisms: Application to hydrogen oxidation in supercritical water. Combust. Flame. 112, 132–146, 1998.
- water, *Combust. Flame*, *112*, 132–146, 1998.

 Pun, B. K., R. J. Griffin, C. Seigneur, and J. H. Seinfeld, Secondary organic aerosol: 2. Thermodynamic model for gas/particle partitioning of molecular constituents, *J. Geophys. Res.*, *107*(D17), 4333, doi:10.1029/2001JD000542, 2002.
- Rabitz, H., and J. Hales, An ACP Primer on sensitivity analysis: Monthly update, *DOE Atmos. Chem. Program, 6 (11)*, pp. 1–7, Battelle Pacific Northwest Labs., Richland, Washington, 1995.
- Rabitz, H., M. Kramer, and D. Docol, Sensitivity analysis in chemical kinetics, Ann. Rev. Phys. Chem., 34, 419–461, 1983.
- Stolarski, R. S., D. M. Butler, and R. D. Rundel, Uncertainty propagation in a stratospheric model: 2. Monte Carlo analysis of imprecisions due to reaction rates, *J. Geophys. Res.*, *83*, 3074–3078, 1978.

 Thompson, A. M., and R. W. Stewart, Effect of chemical kinetic uncertain-
- Thompson, A. M., and R. W. Stewart, Effect of chemical kinetic uncertainties on calculated constituents in a tropospheric photochemical model, *J. Geophys. Res.*, *96*, 13,089–13,108, 1991.
- Vuilleumier, L., J. T. Bamer, R. A. Harley, and N. J. Brown, Evaluation of nitrogen dioxide photolysis rates in an urban area using data from the 1997 Southern California Ozone Study, *Atmos. Environ.*, 35, 6525–6537, 1997
- Yang, Y., W. R. Stockwell, and J. B. Milford, Effect of chemical product yield uncertainties on reactivities of VOCs and emissions from reformulated gasolines and methanol fuels, *Environ. Sci. Technol.*, 29, 1336–1345, 1996.

D. Dabdub and M. A. Rodriguez, Department of Mechanical and Aerospace Engineering, University of California, Irvine, Irvine, CA 92697-3975, USA. (ddabdub@uci.edu)